Spin-polarized tunneling in MgO-based tunnel junctions with superconducting electrodes

2012 New J. Phys. 14 033023

(http://iopscience.iop.org/1367-2630/14/3/033023)

New Journal of Physics
The open-access journal for physics

Spin-polarized tunneling in MgO-based tunnel junctions with superconducting electrodes

Oliver Schebaum[1], Savio Fabretti[1], Jagadeesh S Moodera[2] and Andy Thomas[1,3]

[1] Bielefeld University, Thin Films and Physics of Nanostructures, 33615 Bielefeld, Germany
[2] Francis Bitter Magnet Laboratory, Massachusetts Institute of Technology, Cambridge, MA 02139, USA
E-mail: andy.thomas@uni-bielefeld.de

New Journal of Physics **14** (2012) 033023 (10pp)
Received 9 December 2011
Published 14 March 2012
Online at http://www.njp.org/
doi:10.1088/1367-2630/14/3/033023

Abstract. We prepared magnetic tunnel junctions with one ferromagnetic and one superconducting Al–Si electrode. Pure cobalt electrodes were compared with a Co–Fe–B alloy and the Heusler compound Co_2FeAl. The polarization of the tunneling electrons was determined using the Maki–Fulde model and is discussed along with the spin–orbit scattering and the total pair-breaking parameters. The junctions were post-annealed at different temperatures to investigate the symmetry filtering mechanism responsible for the giant tunneling magnetoresistance ratios in Co–Fe–B/MgO/Co–Fe–B junctions.

Contents

[3] Author to whom any correspondence should be addressed.

1. Introduction

The discovery of the giant magnetoresistance effect in 1988 [1, 2], which led to the realization of room-temperature tunnel magnetoresistance (TMR) of more than a few per cent [3, 4] and the 2007 Nobel prize in Physics for Grünberg and Fert, led to intensive research in the field of spinelectronics or spintronics [5]. Previously, this research was driven by larger and larger TMR-ratios in alumina magnetic tunnel junctions (MTJs), and these have now reached up to 80% at room temperature [6].

In recent years, the search for new material combinations has resulted in increased interest in MgO-based epitaxial MTJs, where large TMR-ratios were predicted and observed due to so-called 'symmetry filtering' [7–10]. Junctions with TMR ratios of up to 600% have been realized in Co–Fe–B/MgO systems [11]. Along this line another system of materials of interest is the class of Heusler compounds, which are predicted to be half-metallic in some cases [12].

Spin-polarized tunneling (SPT) from an electrode into superconducting aluminum was pioneered by Meservey and Tedrow in 1970 [13] and can be seen as a complementary technique to TMR experiments. SPT measurements would be a more direct way to measure the spin polarization (P) of tunneling electrons coming from the ferromagnet than the TMR experiments. If we look only at the TMR ratio and pay no attention to the SPT measurements, one half of the world cannot understand the pleasures of the other. However, only a few experiments with MgO-based systems have been reported [9, 14–16]. In this paper, we present SPT-experimental results on MgO-based junctions with ferromagnetic electrodes such as cobalt, Co–Fe–B and Co_2FeAl (Heusler) and superconducting Al–Si counter electrodes. It was shown that small amounts of Cu or Si can increase the superconducting transition temperature of thin Al films [17]. In our case, a sputter target with a composition of 95% Al and 5% Si resulted in a transition temperature in the range of 2.3–2.7 K, while pure Al exhibited only 2.0 K.

2. Preparation

The samples investigated in the present study were prepared using dc and radio-frequency magnetron sputtering in an automatic sputtering system at ambient temperature. The tunnel junctions were made using molybdenum shadow masks with a cross-strip geometry. The 300 μm width of the strips resulted in a junction area of approximately $9 \times 10^4\ \mu m^2$. To avoid short circuits at the edges of the stripes, the tunnel barrier was sputtered without a shadow mask. After deposition the samples were annealed *ex situ* in a vacuum furnace at various temperatures for 1 h. The base pressure of both the sputtering system and the vacuum furnace was 1×10^{-7} mbar.

The differential conductance dI/dV versus bias voltage V of the S–I–F-tunnel junctions was measured with standard lock-in techniques. The ac excitation voltage was always kept below the thermal smearing threshold $k_B \cdot T$. The measurements were made in ^{3}He cryostats. The Al–Si/MgO/Co samples were measured at the Francis Bitter Magnet Laboratory at a temperature of 0.45 K. All other samples were investigated at Bielefeld University at 0.3 K. While carrying out the measurements, a magnetic field was applied in the plane of the sample to create Zeeman splitting of the superconducting density of states [13].

The transition temperature of the Al–Si/MgO/Co tunnel junction was measured by passing a constant current of 10 μA through the Al–Si strip while measuring the voltage drop across this strip. For the other junctions, the transition temperature of the tunnel junction was determined

by measuring the differential conductance $\mathrm{d}I/\mathrm{d}V$ at $V = 0$ while cooling the sample. At the transition to the superconducting phase, a decrease in the conductance was visible due to the formation of the superconducting energy gap. The error in T_c is ± 0.02 K for both methods.

3. Fitting procedure

The spin polarization, P, of the tunneling current was determined by fitting theoretical curves calculated using the Maki–Fulde theory for a superconductor in a magnetic field [18, 19] to the measured conductances [20]. In addition to P, the parameters for this theory include the measuring temperature T, the energy gap Δ_0, the magnetic field H, the spin–orbit scattering parameter b and the pair-breaking parameter $\zeta(H)$ [21, 22]. For the calculation of the theoretical Maki curves, H and T were kept at their known or measured values and not varied as fitting parameters. The parameters b and P were chosen to fit the curves for the three different magnetic fields with the same set of parameters. Initially, Δ_0 was taken to match the Bardeen–Cooper–Schrieffer (BCS) relation $2\Delta_0 = 3.52 k_B T_c$. However, even pure Al is not an ideal BCS superconductor, as shown by Meservey *et al* [13]. We determined a factor of $3.8 k_B T_c$ for Al–Si, while Meservey *et al* found a value of 3.7 for pure Al. The Maki parameters are shown at the corresponding curves in the figures.

4. Cobalt-based junctions

First, we present the measurements from cobalt junctions with an Al–Si (3.84 nm)/MgO (1.8 nm)/Co (20 nm) layer stack. The results of two different systems are presented: (i) as-prepared and (ii) *ex-situ* annealed at a temperature of $T_a = 325\,^{\circ}$C. The critical temperatures of Al–Si were 2.21 ± 0.12 and 2.41 ± 0.05 K, respectively.

The differential conductance measurements are depicted in figure 1. The Al–Si superconducting energy gaps and the Zeeman splits of Al–Si quasi-particle density of states, as well as the asymmetry of the conductance curves, are apparent. The theoretical fit conductance curves for both samples show good agreement with the data. The spin–orbit scattering parameter, b, is between 0.01 and 0.03 for all measurements and is comparable to the published results for $Al_{98}Si_2$ alloys [9]. The same reference reports pair-breaking parameters in a parallel magnetic field of 2 T between $\zeta = 0.024$ and $\zeta = 0.053$. If we extrapolate our parameters to match the magnetic field of 2 T, our layer stacks show values of $\zeta = 0.048$ and $\zeta = 0.042$ for the as-prepared and annealed samples, respectively. The lower b values for the annealed sample are caused by the increased critical temperature.

The spin polarization of the as-prepared sample was determined to be $P = 32 \pm 2$ and $33 \pm 2\%$ for as-grown and annealed junctions. This value matches the values of $P = 30 \pm 2\%$ that have been reported by Kant *et al* [14]. Both values appear to be low when compared to TMR values of epitaxial Co(001)/MgO(001)/Co(001) junctions. Those annealed junctions exhibit TMR ratios of 410% at room temperature and 507% at low temperatures [23]. The high values can be explained by symmetry filtering [7, 8], which can only occur with ultra-thin, metastable, bcc Co(001) electrodes [24]. However, the molecular beam epitaxy preparation of the junctions utilized by Yuasa *et al* is incompatible with the preparation of SPT samples [9, 25–27].

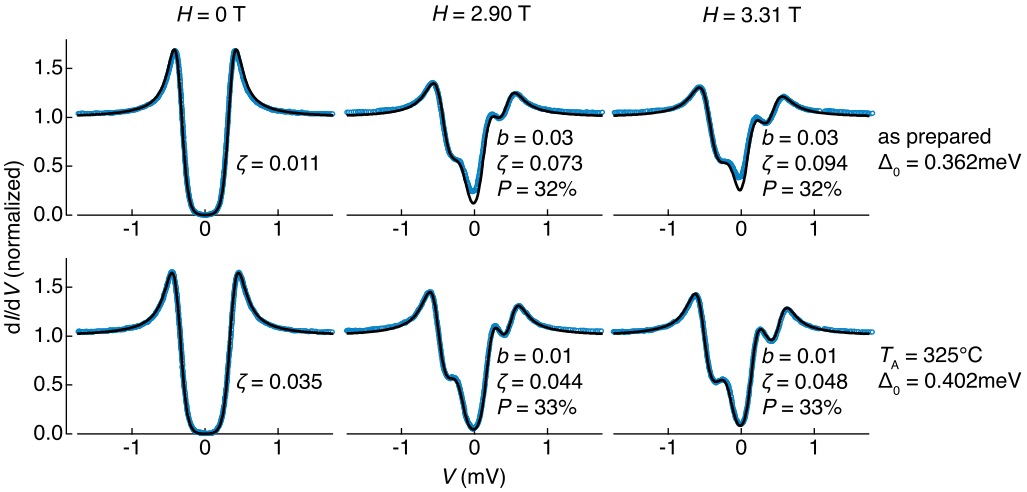

Figure 1. Differential conductivity of a $Al_{95}Si_5$ (3.84 nm)/MgO (1.8 nm)/Co (20 nm) junction. The top row shows the as-prepared sample at different magnetic fields and the bottom row depicts the junction annealed at 325 °C. The measurements and Maki calculations are displayed as blue circles and black lines, respectively.

5. Co–Fe–B-based junctions

MTJs with Co–Fe–B electrodes show the highest TMR ratios. This has been observed in alumina-based junctions where values of up to 80% have been reached [6] and in MgO junctions where a ratio of more than 600% at room temperature has been attained [11]. The control MTJs that are produced in our group using the same sputtering systems as those in the present study reach TMR ratios of 73 and 323% for alumina and MgO tunnel barriers, respectively [28]. The sputtered Co–Fe–B layers are initially amorphous, which is a result of the approximately 20% boron content. A post-annealing temperature of typically more than 250 °C leads to crystallization of the layers [29].

At least two possible mechanisms have been proposed that give rise to the high TMR ratios of the Co–Fe–B alloys. Firstly, the smooth surface of the Co–Fe–B electrodes may improve the layer growth [30]. Secondly, the boron presence may increase the polarization of the tunneling electrons [31]. These were also the motivation for our SPT investigation of Co–Fe–B, complimenting our TMR studies.

Figure 2 displays the differential conductance measurements of the Co–Fe–B samples. Once again the BCS gap in the Al–Si density of states and its asymmetric spin split peaks in a magnetic field are visible. The calculated Maki curves are a good fit for the experimental data. The Al–Si T_c for the annealed samples is higher than for the as-prepared samples. Again, the spin–orbit scattering parameter and the pair breaking parameter are consistent with the values reported in the literature [9]. However, it is interesting to observe the change in the magnitude of the spin polarization values with annealing temperature. The as-prepared sample starts with a ratio of $49 \pm 2\%$, initially drops to $35 \pm 2\%$ at an annealing temperature of $T_a = 310$ °C and continues with a slow increase to $39 \pm 2\%$ for $T_a = 360$ °C.

To rule out that this surprising observation does not originate from the different layer thickness of 20 nm in our case compared with a thickness of 3 nm in most MTJs [11], we

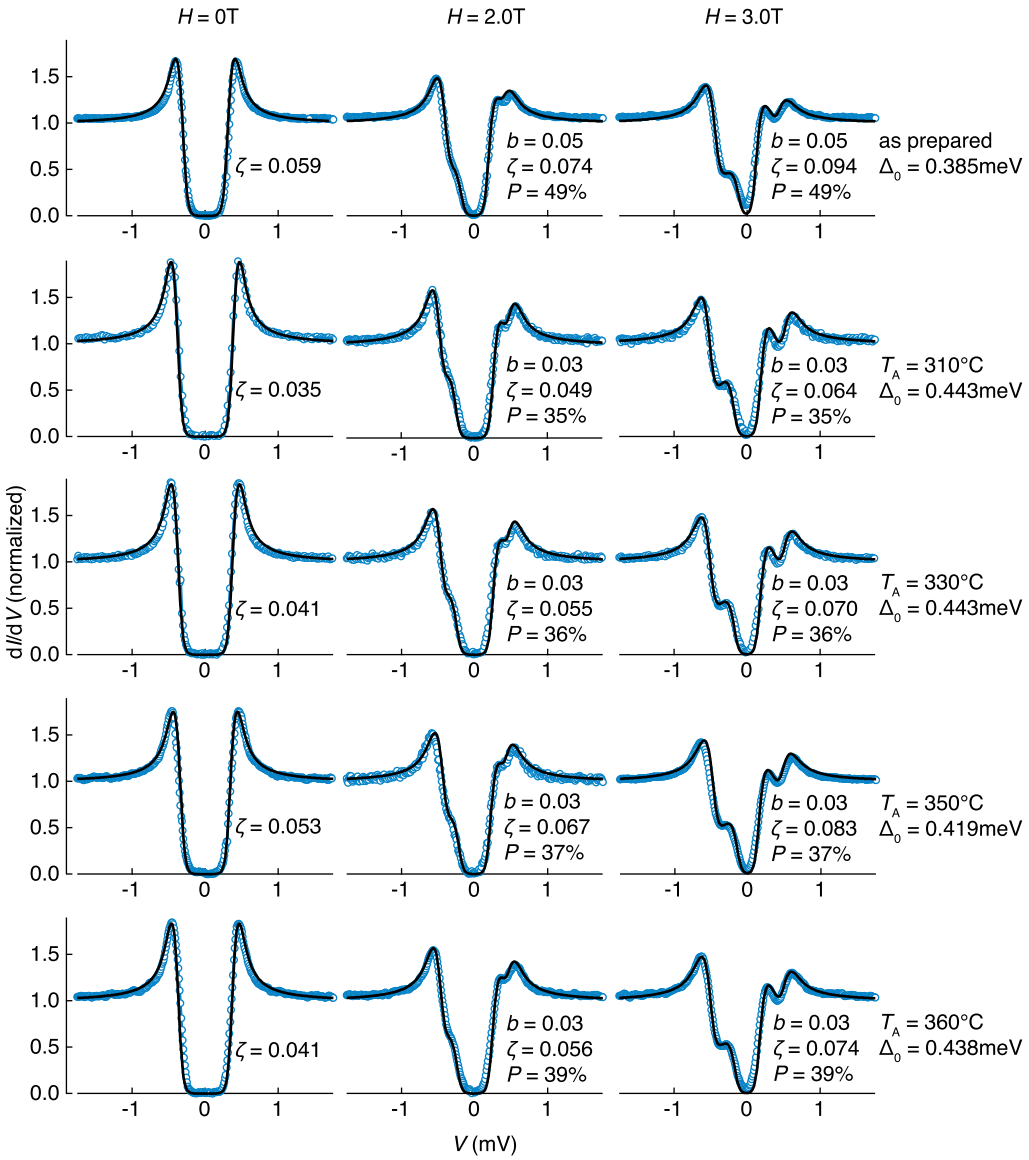

Figure 2. Differential conductance measurements of $Al_{95}Si_5$ (4.0 nm)/MgO (2.1 nm)/ $Co_{40}Fe_{40}B_{20}$ (20 nm) junctions at different external magnetic fields and after various post-annealing temperatures.

then prepared another sample with an $Al_{95}Si_5$ (4.0 nm)/MgO (2.1 nm)/ $Co_{40}Fe_{40}B_{20}$ (3 nm)/Ta (10 nm) layer stack. The additional tantalum layer improves the electrode film conductivity, which otherwise leads to the so-called 'current crowding' effects modifying the transport measurements [3], which could influence the peak heights [27].

The dI/dV measurements of these junctions that were annealed at $T_a = 350\,^{\circ}C$ are depicted in figure 3. In this sample, the spin polarization was increased and showed values of $47 \pm 2\%$, although all other parameters, such as ζ and b, were approximately the same. To explain the results, we divided the spin polarization curve depicted in figure 4 into three parts: the initial drop at $T_a = 310\,^{\circ}C$, the slow increase with further increase in annealing temperature

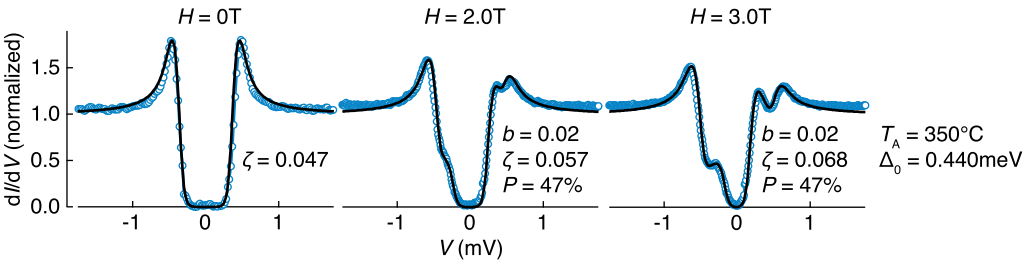

Figure 3. Differential conductance of an $Al_{95}Si_5$ (4.0 nm)/MgO (2.1 nm)/$Co_{40}Fe_{40}B_{20}$ (3 nm)/Ta (10 nm) junction in different magnetic fields. The experimental data are given in blue and the Maki fit is given in black.

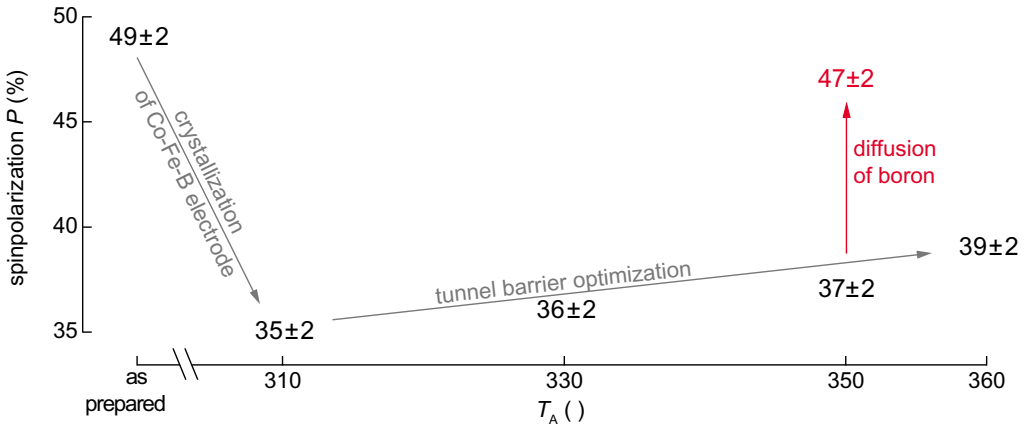

Figure 4. The spin polarization values as a function of the annealing temperature. The arrows indicate the effect of the three different mechanisms explained in the text and their origin.

and the higher values of the Co–Fe–B/Ta double layers. We began with the initial drop of the spin polarization and compared our results to those from alumina-based junctions. We disregarded symmetry filtering effects, which are observed at higher temperatures of more than $T_a = 350\,^{\circ}$C [9]. Gao *et al* [32] have investigated the spin polarization in $Al_{95}Si_5/Al_2O_3$/Co–Fe MTJs. They found a spin polarization of amorphous, ultra-thin Co–Fe electrodes of $P = 55.2\%$, which exceeds the polarization values, $P = 39.1\%$, of the annealed samples. This behavior has also been observed in MTJs [33] and corresponds well to the initial drop of P observed in our experiments.

To investigate the direct influence of the boron aside from the amorphization of the Co–Fe, Paluskar *et al* [31] determined the spin polarization of $Co_{72}Fe_{20}B_8$ electrodes at different layer thicknesses and annealing temperatures. They compared the experimental results with calculations based on density functional theory calculations of electrodes with either a bcc crystal structure or amorphous constitution. In their calculations and in their experiments, Paluskar *et al* also found a lower spin polarization of the tunneling electrons in the junctions with crystalline electrodes compared with junctions with amorphous layer electrodes. If we apply their calculations to our composition of $Co_{40}Fe_{40}B_{20}$, we obtain an expected polarization value of $P = 50.6\%$. This matches our experiments which yield a polarization value of $P = 49 \pm 2\%$. Investigations of the spin polarization of Co–Fe–B electrodes with the point contact Andreev

reflection revealed a lower spin polarization in (partly) crystalline Co–Fe–B compared to amorphous Co–Fe–B [34].

Next, we examined the slow but continuous increase of the spin polarization with increasing the annealing temperatures from $T_a = 310\,^{\circ}\mathrm{C}$ to $T_a = 360\,^{\circ}\mathrm{C}$, which is also depicted in figure 4. Similar experiments with alumina-based junctions have yielded no increase, even for annealing temperatures of up to $T_a = 500\,^{\circ}\mathrm{C}$ [26]. Conversely, MgO-based tunnel junctions show a crystallization of the electrode/MgO interface and therefore an increase of the spin polarization of the tunneling electrons due to symmetry filtering [9]. This increase has also been observed in MTJ(s) with Co–Fe–B electrodes and MgO tunnel barriers: a TMR value of up to 600% has been determined at room temperature [11]. In the present study, the increase in this work can also be attributed to a crystallization of the electrode–barrier interface, although our sample preparation method does not allow for the high annealing temperatures that can lead to polarization values beyond 80% [9].

The mechanism responsible for the higher spin polarization in the junctions with Co–Fe–B/Ta electrodes, as shown in figure 4, is still an open question. Investigations of Co–Fe–B/MgO/Co–Fe–B-MTJ(s) with hard x-ray photo emission spectroscopy (HAXPES) have shown that boron diffusion in the adjacent tantalum layer is responsible for the high TMR-ratios [35]. Although higher annealing temperatures of $T_a = 500\,^{\circ}\mathrm{C}$ were used in the HAXPES experiments, the results suggest that the same mechanism might be responsible for the increase of the tunneling spin polarization in our work.

6. Co_2FeAl-based junctions

Apart from increasing the tunneling spin polarization by symmetry filtering, a second approach to targeting higher TMR ratios is by maximization of the spin polarization of the ferromagnetic electrodes. Half-metallic ferromagnets exhibit the highest possible polarization of 100% [12]; this is predicted for CrO_2 [36], magnetite [37] and Heusler compounds. While the former compounds are fixed in their composition and constituents, the Heusler compounds can be tailored by substitution of the constituents [38, 39].

As shown by Ebke *et al* [40], Co_2FeAl has a low crystallization temperature and yields high TMR ratios when included as a ferromagnetic electrode in MTJs. Therefore, the Heusler compound Co_2FeAl has been investigated. Ebke *et al* [40] have reported that the Heusler compounds in MTJs require a particular layer stack. The electrode had to be grown on a 5 nm MgO buffer on MgO substrates. In our case, this requires an inverted layer stack with the ferromagnetic electrode at the bottom and the superconductor at the top of the system. This inversion and the MgO buffer layer and substrate demand a different thickness of the Al–Si to ensure good superconducting properties of the spin detector. This has also been reported by Yang *et al* [16]. We used a layer stack of MgO (5 nm)/Co_2FeAl (20 nm)/MgO (2.1 nm)/Al_{95}–Si_5 (5 nm) and investigated annealing temperatures of 350 and 375 °C, where the largest change and the highest TMR ratios were found in our earlier experiments [40].

In figure 5, the experimental and the theoretical $\mathrm{d}I/\mathrm{d}V$–V curves of the Co_2FeAl junctions are shown. From the fit of the theoretical to the measured curves, a spin polarization of $59 \pm 2\%$ can be deduced for both the sample annealed at 350 °C and the sample annealed at 375 °C. This is similar to the value $P = 56.2\%$ given by Inomata [41], which was calculated from TMR values of Co_2FeAl/Al_2O_3/Co–Fe MTJs measured at $T = 5$ K. In the same study, a theoretical value of $P = 60.7\%$ for this compound was reported, which is also in good agreement with

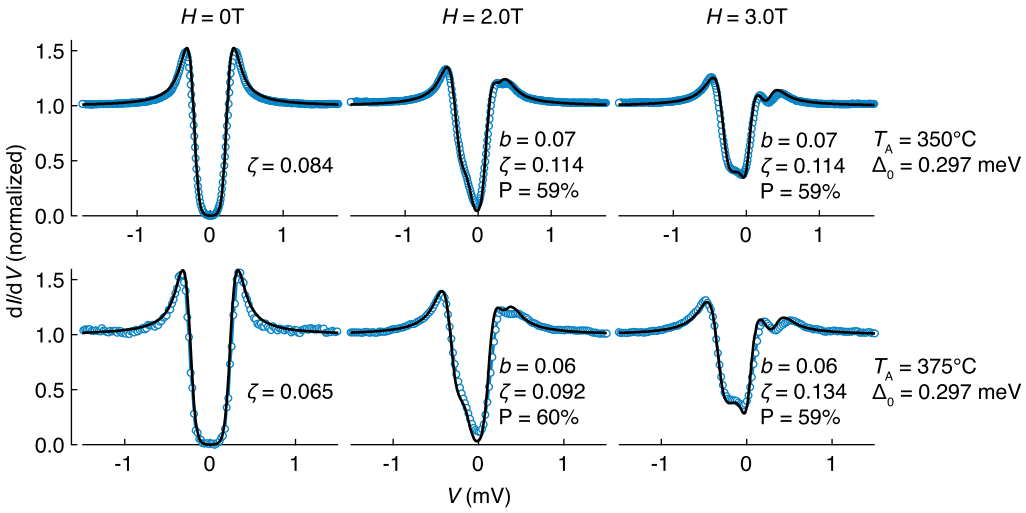

Figure 5. Differential conductance of MgO (5 nm)/Co_2FeAl (20 nm)/MgO (2.1 nm)/AlSi (5 nm) tunnel junctions. The measurements reveal a spin polarization of 59% for both annealing temperatures.

the value obtained in our experiments. Compared to the Co and Co–Fe–B tunnel junctions, higher spin–orbit scattering and pair-breaking values had to be used, as previously seen by Yang *et al* [16] for superconducting Al–Si electrodes on top of an MgO tunnel barrier.

Because of the good agreement between the measured and theoretically predicted spin polarizations, the increase in the TMR ratio can be attributed to symmetry filtering of the tunnel barrier. Additionally, the oscillation of the TMR ratio with increasing MgO thickness in Co_2FeAl/MgO/Co–Fe MTJs that has been found by Wang *et al* [42] suggests that the high TMR ratios in MTJs containing Co_2FeAl are based on symmetry filtering rather than highly spin-polarized electrodes.

7. Summary

We investigated the transport properties of tunnel junctions with a magnetic electrode and a superconducting Al–Si counter electrode with and without magnetic fields for different post-annealing temperatures. This included the measurement of spin polarization by the Meservey–Tedrow technique. We evaluated the spin polarization as well as the spin–orbit scattering and total pair-breaking parameter using the Maki–Fulde model, and we compared the data with the corresponding MTJs. These two techniques complement each other to provide a better understanding of the underlying physics. In the future, samples with superconducting counter electrodes and prepared with a lithographic process similar to that used to produce MTJs would be useful.

Acknowledgments

We gratefully thank Th Dahm and G Reiss for fruitful discussions. O, S and A acknowledge the Ministerium für Innovation, Wissenschaft und Forschung of the NRW state government for financial support. JS acknowledges financial support from NSF grant DMR 0504158 and ONR grant N00014-09-1-0177.

References

[1] Baibich M N, Broto J M, Fert A, Nguyen Van Dau F, Petroff F, Eitenne P, Creuzet G, Friederich A and Chazelas J 1988 Giant magnetoresistance of (001)Fe/(001)Cr magnetic superlattices *Phys. Rev. Lett.* **61** 2472–5

[2] Binasch G, Grünberg P, Saurenbach F and Zinn W 1989 Enhanced magnetoresistance in layered magnetic structures with antiferromagnetic interlayer exchange *Phys. Rev.* B **39** 4828–30

[3] Moodera J S, Kinder L R, Wong T M and Meservey R 1995 Large magnetoresistance at room temperature in ferromagnetic thin film tunnel junctions *Phys. Rev. Lett.* **74** 3273–6

[4] Miyazaki T and Tezuka N 1995 Giant magnetic tunneling effect in Fe/Al_2O_3/Fe junction *J. Magn. Magn. Mater.* **139** L231–4

[5] Prinz G A 1998 Magnetoelectronics *Science* **27** 1660–3

[6] Wei H X, Qin Q H, Ma M, Sharif R and Han X F 2007 80% tunneling magnetoresistance at room temperature for thin Al–O barrier magnetic tunnel junction with CoFeB as free and reference layers *J. Appl. Phys.* **101** 09B501

[7] Butler W, Zhang X, Schulthess T and MacLaren J 2001 Spin-dependent tunneling conductance of Fe/MgO/Fe sandwiches *Phys. Rev.* B **63** 054416

[8] Mathon J and Umerski A 2001 Theory of tunneling magnetoresistance of an epitaxial Fe/MgO/Fe (0 0 1) junction *Phys. Rev.* B **63** 220403

[9] Parkin S S P, Kaiser C, Panchula A, Rice P M, Hughes B, Samant M and Yang S 2004 Giant tunnelling magnetoresistance at room temperature with MgO (1 0 0) tunnel barriers *Nature Mater.* **3** 862–7

[10] Yuasa S, Nagahama T, Fukushima A, Suzuki Y and Ando K 2004 Giant room-temperature magnetoresistance in single-crystal Fe/MgO/Fe magnetic tunnel junctions *Nature Mater.* **3** 68–71

[11] Ikeda S, Hayakawa J, Ashizawa Y and Lee Y 2008 Tunnel magnetoresistance of 604% at 300 K by suppression of Ta diffusion in CoFeB/MgO/CoFeB pseudo-spin-valves annealed at high temperature *Appl. Phys. Lett.* **93** 082508

[12] R A de Groot, Mueller F M, van Engen P G and Buschow K H J 1983 New class of materials: half-metallic ferromagnets *Phys. Rev. Lett.* **50** 2024–7

[13] Meservey R, Tedrow P M and Fulde P 1970 Magnetic field splitting of the quasiparticle states in superconducting aluminum films *Phys. Rev. Lett.* **25** 1270–2

[14] Kant C H, Kohlhepp J, Swagten H and Koopmans B 2004 Role of the barrier in spin-dependent tunneling addressed with superconductor spectroscopy *Phys. Rev.* B **69** 172408

[15] Yang H, Yang S H, Kaiser C and Parkin S S P 2006 Tunneling spin polarization measurements from ferromagnet/MgO tunnel junctions using NbN superconductor *Appl. Phys. Lett.* **88** 182501

[16] Yang H, Yang S H, Parkin S S P, Leo T and Smith D J 2007 Optimized thickness of superconducting aluminum electrodes for measurement of spin polarization with MgO tunnel barriers *Appl. Phys. Lett.* **90** 202502

[17] Monsma D J and Parkin S S P 2000 Spin polarization of tunneling current from ferromagnet/Al_2O_3 interfaces using copper-doped aluminum superconducting films *Appl. Phys. Lett.* **77** 720–2

[18] Maki K 1964 Pauli paramagnetism and superconducting state II *Prog. Theor. Phys.* **32** 29–36

[19] Fulde P 1973 High field superconductivity in thin films *Adv. Phys.* **22** 667–719

[20] Alexander J, Orlando T, Rainer D and Tedrow P M 1985 Theory of Fermi-liquid effects in high-field tunneling *Phys. Rev.* B **31** 5811–25

[21] Meservey R and Tedrow P M 1994 Spin-polarized electron tunneling *Phys. Rep.* **238** 173–243

[22] Worledge D C and Geballe T H 2000 Maki analysis of spin-polarized tunneling in an oxide ferromagnet *Phys. Rev.* B **62** 447–51

[23] Yuasa S, Fukushima A, Kubota H, Suzuki Y and Ando K 2006 Giant tunneling magnetoresistance up to 410% at room temperature in fully epitaxial Co/MgO/Co magnetic tunnel junctions with bcc Co (0 0 1) electrodes *Appl. Phys. Lett.* **89** 042505

[24] Bagayako D, Ziegler A and Callaway J 1983 Band structure of bcc cobalt *Phys. Rev.* B **27** 7046–9

[25] Tanaka C T, Nowak J and Moodera J S 1999 Spin-polarized tunneling in a half-metallic ferromagnet *J. Appl. Phys.* **86** 6239–42
[26] Kant C H, Kohlhepp J T, Swagten H J M and de Jonge W J M 2004 Intrinsic thermal robustness of tunneling spin polarization in $Al/Al_2O_3/Co$ junctions *Appl. Phys. Lett.* **84** 1141–3
[27] Worledge D C and Geballe T H 2000 Spin-polarized tunneling in $La_{0.67}Sr_{0.33}MnO_3$ *Appl. Phys. Lett.* **76** 900–2
[28] Schebaum O, Drewello V, Auge A, Reiss G, Münzenberg M, Schuhmann H, Seibt M and Thomas A 2011 Tunnel magnetoresistance in alumina, magnesia and composite tunnel barrier magnetic tunnel junctions *J. Magn. Magn. Mater.* **323** 1525–8
[29] Paluskar P V, Kohlhepp J T, Swagten H and Koopmans B 2006 $Co_{72}Fe_{20}B_8$: structure, magnetism and tunneling spin polarization *J. Appl. Phys.* **99** 08E503
[30] Yuasa S and Djayaprawira D D 2007 Giant tunnel magnetoresistance in magnetic tunnel junctions with a crystalline MgO(0 0 1) barrier *J. Phys. D: Appl. Phys.* **40** R337–54
[31] Paluskar P V, Attema J J, de Wijs G A, Fiddy S, Snoeck E, Kohlhepp J T, Swagten H, de Groot R A and Koopmans B 2008 Spin tunneling in junctions with disordered ferromagnets *Phys. Rev. Lett.* **100** 1–4
[32] Gao L, Jiang X, Rice P M and Parkin S S P 2009 Enhanced tunneling spin polarization from ultrathin layers of amorphous CoFe *Appl. Phys. Lett.* **95** 122503
[33] Gao L, Jiang X, Yang S-H, Rice P, Topuria T and Parkin S S P 2009 Increased tunneling magnetoresistance using normally bcc CoFe alloy electrodes made amorphous without glass forming additives *Phys. Rev. Lett.* **102** 247205
[34] Huang S X, Chen T Y and Chien C L 2008 Spin polarization of amorphous CoFeB determined by point-contact Andreev reflection *Appl. Phys. Lett.* **92** 242509
[35] Kozina X, Ouardi S, Balke B, Stryganyuk G, Fecher G H, Felser C, Ikeda S, Ohno H and Ikenaga E 2010 A nondestructive analysis of the B diffusion in Ta–CoFeB–MgO–CoFeB–Ta magnetic tunnel junctions by hard x-ray photoemission *Appl. Phys. Lett.* **96** 072105
[36] Schwarz K 1986 CrO_2 predicted as a half-metallic ferromagnet *J. Phys. F: Met. Phys.* **16** L211–5
[37] Pénicaud M, Siberchicot B, Sommers C B and Kübler J 1992 Calculated electronic band structure and magnetic moments of ferrites *J. Magn. Magn. Mater.* **103** 212–20
[38] Balke B, Wurmehl S, Fecher G H, Felser C and Kübler J 2008 Rational design of new materials for spintronics: Co_2FeZ(Z = Al, Ga, Si, Ge) *Sci. Tech. Adv. Mater.* **9** 014102
[39] Ebke D, Schmalhorst J, Liu N-N, Thomas A, Reiss G and Hütten A 2006 Large tunnel magnetoresistance in tunnel junctions with Co_2MnSi/Co_2FeSi multilayer electrode *Appl. Phys. Lett.* **89** 162506
[40] Ebke D, Thomas P, Schebaum O, Schäfers M, Nissen D, Drewello V, Hütten A and Thomas A 2010 Low $B2$ crystallization temperature and high tunnel magnetoresistance in Co_2FeAl/MgO/Co–Fe magnetic tunnel junctions *J. Magn. Magn. Mater.* **322** 996–8
[41] Inomata K, Ikeda N, Tezuka N and Goto R 2008 Highly spin-polarized materials and devices for spintronics *Sci. Technol. Adv. Mater.* **9** 014101
[42] Wang W, Liu E, Kodzuka M, Sukegawa H, Wojcik M, Jedryka E, Wu G H, Inomata K, Mitani S and Hono K 2010 Coherent tunneling and giant tunneling magnetoresistance in $Co_2FeAl/MgO/CoFe$ magnetic tunneling junctions *Phys. Rev.* B **81** 140402